Published online 6 March 2013 *Nucleic Acids Research, 2013, Vol. 41, No. 8* ***4535–4548***
doi:10.1093/nar/gkt154

Concurrent V(D)J recombination and DNA end instability increase interchromosomal *trans*-rearrangements in ATM-deficient thymocytes

Steven Bowen[1,2,*], Darawalee Wangsa[3], Thomas Ried[3], Ferenc Livak[4] and Richard J. Hodes[2]

[1]Department of Microbiology and Immunology, Graduate Program in Life Sciences, University of Maryland Baltimore, Baltimore, MD 21201, USA, [2]Experimental Immunology Branch, National Cancer Institute, National Institute of Health, Bethesda, MD 20892, USA, [3]Genetics Branch, National Cancer Institute, National Institute of Health, Bethesda, MD 20892, USA and [4]Marlene and Stuart Greenebaum Cancer Center, University of Maryland, Baltimore, MD 21201, USA

Received January 30, 2013; Revised February 14, 2013; Accepted February 15, 2013

ABSTRACT

During the CD4$^-$CD8$^-$ (DN) stage of T-cell development, RAG-dependent DNA breaks and V(D)J recombination occur at three T-cell receptor (TCR) loci: TCRβ, TCRγ and TCRδ. During this stage, abnormal *trans*-rearrangements also take place between TCR loci, occurring at increased frequency in absence of the DNA damage response mediator ataxia telangiectasia mutated (ATM). Here, we use this model of physiologic *trans*-rearrangement to study factors that predispose to rearrangement and the role of ATM in preventing chromosomal translocations. The frequency of DN thymocytes with DNA damage foci at multiple TCR loci simultaneously is increased 2- to 3-fold in the absence of ATM. However, *trans*-rearrangement is increased 10 000- to 100 000-fold, indicating that ATM function extends beyond timely resolution of DNA breaks. RAG-mediated synaptic complex formation occurs between recombination signal sequences with unequal 12 and 23 base spacer sequences (12/23 rule). TCR *trans*-rearrangements violate this rule, as we observed similar frequencies of 12/23 and aberrant 12/12 or 23/23 recombination products. This suggests that *trans*-rearrangements are not the result of *trans*-synaptic complex formation, but they are instead because of unstable *cis* synaptic complexes that form simultaneously at distinct TCR loci. Thus, ATM suppresses *trans*-rearrangement primarily through stabilization of DNA breaks at TCR loci.

INTRODUCTION

DNA double-strand breaks (DSBs) are the most hazardous type of lesion encountered by the genome because of their susceptibility to potentially oncogenic mutations. To prevent genomic instability, a highly efficient DNA damage response (DDR) has evolved to facilitate the recognition and repair of DSBs. V(D)J recombination in developing lymphocytes assembles the genes encoding the variable domain of the antigen-specific T-cell receptor (TCR) and immunoglobulin receptors from discontinuous V, D and J gene segments. This process is tightly regulated and occurs only at specific loci during precise stages of lymphocyte development. The complex of recombination-activating gene proteins RAG-1 and RAG-2 (hereafter referred to as RAG) binds to specific recombination signal sequences (RSSs) flanking each V, D and J gene segment and introduces transient DSBs that activate the DDR pathway and are repaired by the non-homologous end-joining apparatus (1).

The RSS is composed of a gene-proximal heptamer and gene-distal nonamer, both of which are well conserved between gene segments, as well as a non-conserved spacer sequence of either 12 or 23 bp. Through interactions between RAG heterodimers bound to RSSs of unequal spacer length (known as the 12/23 rule), two gene segments are brought together in a synaptic complex, and the DNA is cleaved in a RAG-dependent manner (2–4). During T lymphocyte development, three of the four TCR loci (TCRβ, TCRγ and TCRδ) undergo rearrangement in CD4/CD8 double negative (DN) stage 3 (DN3) cells (5), whereas TCRα recombination occurs in the subsequent CD4/CD8 double positive stage. Importantly, it has not been determined whether

*To whom correspondence should be addressed. Tel: +1 301 451 2103; Fax: +1 301 496 0887; Email: bowense@mail.nih.gov

RAG-dependent breaks and rearrangement occur simultaneously at multiple loci in individual DN3 cells.

The DSBs induced by RAG during lymphocyte development activate the PI3-like kinase ataxia telangiectasia mutated (ATM). The importance of ATM in maintaining the efficiency and fidelity of V(D)J recombination is evidenced by the gross chromosomal abnormalities associated with antigen receptor loci in ATM−/− mice and in human patients with ataxia telangiectasia (AT), an inherited disorder caused by homozygous mutation of the ATM gene (6–8). Two of these abnormalities, first observed in peripheral T cells from human AT patients, were translocations involving chromosome 7 (where the TCRβ and TCRγ loci are located) and chromosome 14 (where the TCRα/δ locus is located) (6,9). Both of these abnormal events represent authentic joints between two different TCR loci and are called *trans*-rearrangements (9–12). During V(D)J recombination in mice, ATM deficiency results in a dramatic increase in improper coding end-signal end rearrangements (referred to as hybrid joints), further suggesting that ATM plays a role in stabilizing RAG–DNA complexes (13,14). ATM is a multifunctional molecule involved in the physical stabilization of broken DNA ends, recruitment of repair factors to allow rapid resolution of DSBs and activation of effector molecules involved in cell cycle checkpoint maintenance and apoptosis (15). ATM has also been implicated in the spatial separation of rearranging antigen receptor loci within the interphase nuclei of developing lymphocytes (16). The relative importance of each of ATM's distinct functions in suppressing chromosomal aberrations is not well understood. Here, we have used TCR *trans*-rearrangements as a model to study the relative contributions of ATM's multiple functions in the prevention of chromosomal translocations.

We demonstrate that ATM−/− mice have an increased frequency of TCRβ/TCRγ *trans*-rearrangement in DN2/3 thymocytes, and that these *trans*-rearrangements persist in mature peripheral T cells. Using combined immunofluorescence/fluorescent *in situ* hybridization (ImmunoFISH), as well as 3D FISH, we show simultaneous DNA DSB break foci at TCRβ, TCRγ and TCRα/δ loci in individual DN2/3 thymocytes from wild-type (WT) and ATM−/− mice. The increased temporal coincidence of DNA break foci, but not changes in spatial subnuclear localization, corresponds with the increased incidence of *trans*-rearrangements in ATM-deficient thymocyte precursors. Strikingly, however, we find that although ATM deficiency results in a modest 2-fold increase of 53BP1 DNA damage foci at any TCR locus and a 3-fold increase in the number of cells with 53BP1 foci at two or more TCR loci, the frequency of *trans*-recombination is dramatically increased 10 000- to 100 000-fold. The function of ATM in suppressing chromosomal translocations thus seems to extend beyond the timely resolution of DNA breaks. We in fact find that many combinations of *trans*-rearrangements *in vivo* do not obey the 12/23 rule, suggesting that post-cleavage DNA breaks are particularly unstable in the absence of ATM, and that recombination occurs between unstable DNA ends rather than RAG-dependent synapsis in *trans* between two different loci. ATM thus functions to protect antigen receptor loci from abnormal recombination both by facilitating the timely repair of DNA breaks, and to an even greater extent by physically stabilizing DNA ends after RAG-mediated cleavage.

MATERIALS AND METHODS

Mice

ATM−/− mice were generated through a mutation of the ATM gene at nucleotide 5790 resulting in a truncation of the protein (17). ATM+/− breeders were used to generate ATM−/− progeny, as well as ATM+/+ littermates that were used as WT control mice. All analyses were done at age 6–12 weeks. Animals were maintained at Bioqual (Rockville, MD, USA), and all procedures were approved by the National Cancer Institute Animal Care and Use Committee.

Cell purification

DN2/3 thymocytes were flow sorted by gating on thymocytes negative for the following biotinylated lineage-specific antibodies: TCRβ (H57-597), CD4, CD8, B220, natural killer 1.1, MAC1, GR-1 and GL3 (BD Biosciences, San Jose, CA, USA) and positive for CD25 (BD Biosciences). Each DN2/3 sample was prepared from a pool of five to eight mice of each genotype. Peripheral T cells were flow sorted by gating on B220−, TCRβ (H57-597)+ splenocytes. Each peripheral T-cell sample was prepared from one individual mouse. All sorting was done on a FACSAria cell sorter (BD Biosciences, San Jose, CA, USA).

Standard polymerase chain reaction analysis of TCR *trans*-rearrangement

Genomic DNA was purified from sorted DN2/3 thymocytes and peripheral T cells using a DNeasy Blood and Tissue Kit (Qiagen, Valencia, CA, USA). The following primers were used to amplify Vγ–Jβ *trans*-rearrangements: GV2F1; 5′-AAAATGGAGGCAAGTAAAAATCC-3′, 3Jb1b; 5′-TAGGTTTACAACACACCCTCCCGAG-3′, 3Jb2; 5′-CCAGGAATTTGGGTGGAAGCGAG-3′. Reactions for Vγ2–Jβ *trans*-rearrangements were performed on 100, 20 and 4 ng of genomic DNA. The following primers were used with GV4F1 to amplify Dβ–Vγ2 *trans*-rearrangements: 5Db1SE; 5′-GGTAAAGAGGAA ACCCCTGCATTAGC-3′, 5Db2SE; 5′-TGCCACCTGG TCTCCCTGCCCCTG-3′. To amplify Jγ1–Jβ *trans*-rearrangements, the following primer was used with 3Jb1b and 3Jb2: GJ1R1; 5′-TTCCTATGAGCTTAGTTCCTTC TG-3′. Reactions for Jγ–Jβ and Dβ–Vγ rearrangements were performed on 100 ng of genomic DNA. All polymerase chain reactions (PCR) were done with JumpStart Taq ReadyMix (Sigma, St. Louis, MO, USA).

Real-time PCR analysis of TCR *trans*-rearrangement

A 20 cycle pre-amplification reaction was performed using GV4F1 and either 3Jb1b or 3Jb2. The reaction was diluted 500-fold and used as a template for real time PCR. GV4F1

was used as a forward primer to amplify individual Vγ–Jβ rearrangements using the following nested reverse primers: BJ1.1R1; 5′-ACTGTGAGTCTGGTTCCTTTACC-3′, BJ2.7R1; 5′-CTAAAACCGTGAGCCTGGTGC-3′. Reactions were run on a 7900HT Fast Real Time PCR System (Life Technologies, Carlsbad, CA, USA) using RT^2 SYBR Green qPCR Mastermix (SA Biosciences, Valencia, CA, USA), and data were collected and analyzed with SDS 2.3 software (Life Technologies). Each Vγ–Jβ reaction was normalized to control amplification on the same DNA sample of an invariant non-rearranging region of the TCRα locus (Cα) using the following formula: $1.9^{-\mathrm{CtVg\text{-}Jb}}/1.9^{-\mathrm{CtC\alpha}}$. The normalized values were averaged between five independent experiments, and statistical significance was calculated using a paired student's *t*-test. Amplification products were verified by dissociation curve analysis and gel electrophoresis.

For the quantitation of 12/12 versus 12/23 *trans*-rearrangement, 60 ng of genomic DNA purified from flow-sorted DN2/DN3 thymocytes was pre-amplified for 20 cycles with either GJ1R1 or GV2F1 as a forward primer and 3Jb2 as a reverse primer. The pre-amplified product was diluted 500-fold for the real-time PCR. The forward primers for the real-time reaction were either GJ1R1 or GV2F1, and the reverse primer for all reactions was BJ2.7R1. To create a standard curve, Jγ1–Jβ2.7 and Vγ2–Jβ2.7 *trans*-rearrangement sequences were TA cloned into the pCR2.1 vector, and the number of molecules per volume was calculated from the molecular weight of the construct. Ten-fold dilutions starting from 1×10^7 molecules per reaction were used to create the standard curve. Linear regression analysis was used to fit our experimental values to the standard curve.

Chromosome painting

Splenocytes from WT and ATM−/− mice were stimulated *in vitro* with anti-CD3 (2C11) + interleukin-2 for 48 h. Metaphase spreads were prepared by Colcemid (Roche, Branchburg, NJ, USA) treatment followed by hypotonic (0.075 M KCl) incubation. This was followed by fixation in methanol and acetic acid (3:1) before being dropped onto Shandon Cytoslides (Thermo Fisher Scientific, Rockville, MD, USA) in a humidified chamber.

Triple color mouse whole chromosome paints were generated in-house using PCR labeling techniques. Chromosome 6 was labeled with Spectrum Orange (Abbott Laboratories), chromosome 13 with Dy505 (Dyomics, Jena, Germany) and chromosome 14 with biotin dUTP (Roche).

Hybridization and detection of chromosome-specific paints were performed as previously described (18). Probes labeled with biotin were detected with Avidin Cy5 (Jackson ImmunoResearch Laboratories, West Grove, PA, USA). Imaging was done with a Zeiss Axio Imager microscope. More than 1000 metaphases for each genotype were detected and imaged using Metafer software (MetaSystems, Boston, MA, USA).

Once imaging was completed, the slides were re-hybridized using a previously described protocol (19). The slides were denatured at 65°C for 20 s before being dehydrated in an ethanol series.

The second probe combination consisted of the following: 3′-TCRβ and 5′-TCRβ probes labeled in Dy505 (Dyomics Jena, Germany); 3′-TCRα/δ and 5′-TCRα/δ probes labeled with Spectrum Orange (Abbott Molecular); 3′-TCRγ and 5′-TCRγ labeled with biotin (Roche). Probes were denatured at 80°C for 5 min then pre-annealed for 1 h before being applied to the slide for overnight hybridization at 37°C. Hybridization and detection of chromosome-specific paints were performed as previously described (18). Probes labeled with biotin were detected with Avidin Cy5 (Jackson ImmunoResearch Laboratories, West Grove, PA, USA).

Immuno FISH analysis

Immunoflourescence for DNA damage foci was combined with FISH as previously described (20). Slides were stained with a rabbit anti-53BP1 (Novus) primary antibody followed by goat anti-rabbit IgG1 conjugated to Alexa-568 (Life Technologies). DNA probes labeled with dUTPs conjugated to biotin (Roche), digoxigenin (Roche) or Cy5 (GE Healthcare, Vienna, VA, USA) were denatured and hybridized to the slides overnight at 37°C. DNA probes were then stained with streptavidin-Alexa 405 (Life Technologies) and anti-digoxigenin conjugated to fluorescein (Roche).

The following BAC constructs obtained from the Childrens Hospital of Oakland Research Institute (CHORI) were used to generate labeled probes by nick translation: 3′-TCRβ; RP24 299 B14, 3′-TCRα/γ; RP23 465 I7, 3′-TCRγ; RP23 306 G1. Imaging was performed on a Zeiss Meta confocal microscope using LSM imaging software and Imaris software (Bitplane Scientific Software). Co-localization of 53BP1 foci was determined by blinded scoring analysis.

3D FISH analysis of DN2/3 thymocytes

Cells were prepared and hybridized as previously described (21). DNA probes were labeled with dUTPs conjugated to biotin (Roche), digoxigenin (Roche), Spectrum Orange (Enzo Life Sciences, Farmingdale, NY, USA) or Cy5 (GE Healthcare) and hybridized to electronically sorted DN2/3 thymocytes. Imaging was performed on a Zeiss Meta confocal microscope using LSM imaging software. Single cells were isolated from fields and imported into the Imaris (Bitplane Scientific Software) imaging program, where the center of homogeneous mass was calculated for each individual FISH signal. Using the *x*, *y* and *z* coordinates obtained, distances between spots were calculated using the following formula for Euclidian distance in 3D space: $\sqrt{(X1-X2)^2+(Y1-Y2)^2+(Z1-Z2)^2}$ where X, Y and Z denote the spatial coordinates within the nucleus for Spot 1 and Spot 2.

The following BAC constructs were used to generate labeled probes by nick translation: 3′-TCRβ; RP24 299 B14, 3′-TCRα/δ; RP23 465 I7, 3′-TCRγ; RP23 306 G1, b Actin; RP23 97 O1 (CHORI).

In vitro recombination assay

Artificial recombination substrates were cloned onto a cytomegalovirus plasmid and co-transfected along with constructs containing RAG1 and RAG2 into HEK293 cells using Lipofectamine LTX (Life Technologies) and incubated at 37°C for 36 h. Cells were harvested and plasmid DNA was extracted. The recombined insert was PCR amplified using primers specific for the flanking sides of the cytomegalovirus backbone. PCR products were run on a 1.5% sieving agarose gel and stained with ethidium bromide to detect DNA.

RESULTS

Trans-rearrangement between TCRβ and TCRγ occurs in DN2/DN3 thymocytes

The DN2/DN3 stage of thymocyte development is unique in that RAG-induced DSBs occur during rearrangements at this developmental period in three unlinked TCR loci, TCRβ, TCRγ and TCRδ. This raises the risk of recombination between different rearranging TCR loci, leading to chromosomal translocations. Such translocations have in fact been described, and they occur at greatly increased frequency in lymphocytes from ATM-deficient mice, where sensing and repair of DSB is impaired (7,8). However, it is not clear whether these translocations occur at the time of recombination in DN2/3 cells or at a later stage of development because of the impaired resolution of DSB, as was suggested to happen at the IgH locus (22). We explored this question by first probing for the existence of *trans*-rearrangements between TCRβ and TCRγ (on mouse chromosomes 6 and 13, respectively), two loci known to undergo physiologic recombination during the DN2/3 stage (5). We analyzed DN2/3 thymocytes from WT and ATM−/− mice by quantitative real-time PCR with a forward primer specific for the Vγ2 gene and reverse primers for individual Jβ genes within the first and second Jβ clusters (Figure 1B). Vγ–Jβ *trans*-rearrangements were detectable in genomic DNA from WT DN2/DN3 thymocytes, and they occurred at a 10 000- to 100 000-fold higher frequency in ATM−/− thymocytes. Similar results were obtained using standard PCR amplification with a Vγ2 forward primer and a reverse primer that amplifies the entire Jβ1 or Jβ2 clusters from serially diluted genomic DNA from WT and ATM−/− samples (Figure 1A). DNA sequencing of the PCR products confirmed that the *trans*-rearranged joints resembled *bona fide* V(D)J recombination products with the presence of N nucleotides at the junctions and small deletions in the coding flanks (Supplementary Table S1). These data indicate that *trans*-rearrangements between TCRβ and TCRγ occur in WT thymocytes, and at much higher frequencies in ATM−/− mice, in DN2/DN3 cells at the time when these TCR loci normally undergo recombination.

TCR *trans*-rearrangements are present in peripheral T lymphocytes

It is possible that cells that generate TCR *trans*-rearrangements early in T-cell development do not survive thymic selection and thus would not be found in the periphery. To test this, we isolated genomic DNA from splenocytes of WT and ATM−/− mice and performed real-time and standard PCR to detect *trans*-rearrangements. Similar to what was observed in DN2/DN3 thymocytes, *trans*-rearrangements involving both Jβ1 and Jβ2 were clearly detectable in ATM−/− splenocytes and at significantly lower levels in the WT sample (Figure 1C and D). These data suggest that not only do *trans*-rearrangements between TCRβ and TCRγ exist in the thymus during early T-cell development, but that cells carrying these translocations can pass through positive and negative thymic selection and exist in the periphery as mature T lymphocytes.

From this PCR analysis, it is not possible to determine the absolute frequency of cells carrying *trans*-rearrangements in the periphery of WT and ATM−/− mice. To analyze the presence of *trans*-rearrangements at the single-cell level, we used whole chromosome painting of WT and ATM−/− colcemid-arrested splenocytes that had been stimulated *in vitro* for 48 h with anti-CD3 and interleukin-2. Paints specific for chromosomes 6, 13 and 14 (the locations of TCRβ, TCRγ and TCRδ, respectively) were hybridized to chromosome spreads to assess the integrity of these chromosomes. The ATM−/− sample contained translocations between all three TCR chromosome combinations [t(6,13) 0.52% (Figure 2A and E), t(13,14) 1.04% (Figure 2B and E) and t(6,14) 1.30% (Figure 2C and E)], and in some cases, multiple translocations were found within a single metaphase (Figure 2D). Both reciprocal and non-reciprocal translocations were observed. A total of 2.85% of ATM−/− splenic T cells carried a chromosomal translocation consistent with a TCR *trans*-rearrangement. To verify that the translocation breakpoints were at the TCR loci, the painted metaphases were re-hybridized with probes specific for the 5′- and 3′-ends of each TCR locus. In all cases, the translocation breakpoints corresponded to the TCR loci (Supplementary Figure S1). No translocations were detected in >1000 WT metaphases analyzed.

DNA break foci occur concurrently at TCRβ, TCRγ and TCR*δ* loci in individual DN2/DN3 thymocytes

It has previously been reported that RAG-dependent DNA breaks occur at TCRβ, TCRγ and TCRδ loci in DN2/DN3 thymocytes (5). However, it has not been determined whether breaks at multiple loci coexist concurrently in individual DN thymocytes. To address the question of whether individual DN2/DN3 thymocytes rearrange multiple TCR loci simultaneously, we used a four-color immune FISH approach, which allows visualization of DNA damage at specific TCR loci by fluorescence microscopy. Immunofluorescent staining for 53BP1, a DDR molecule that forms foci at sites of DNA DSBs, was performed in conjunction with FISH using probes specific for the 3′-regions of the TCRβ, TCRγ and TCRδ loci. Using this approach we are able to simultaneously detect the three TCR loci, as well as foci formed by 53BP1. We analyzed 53BP1 foci because it has been reported that

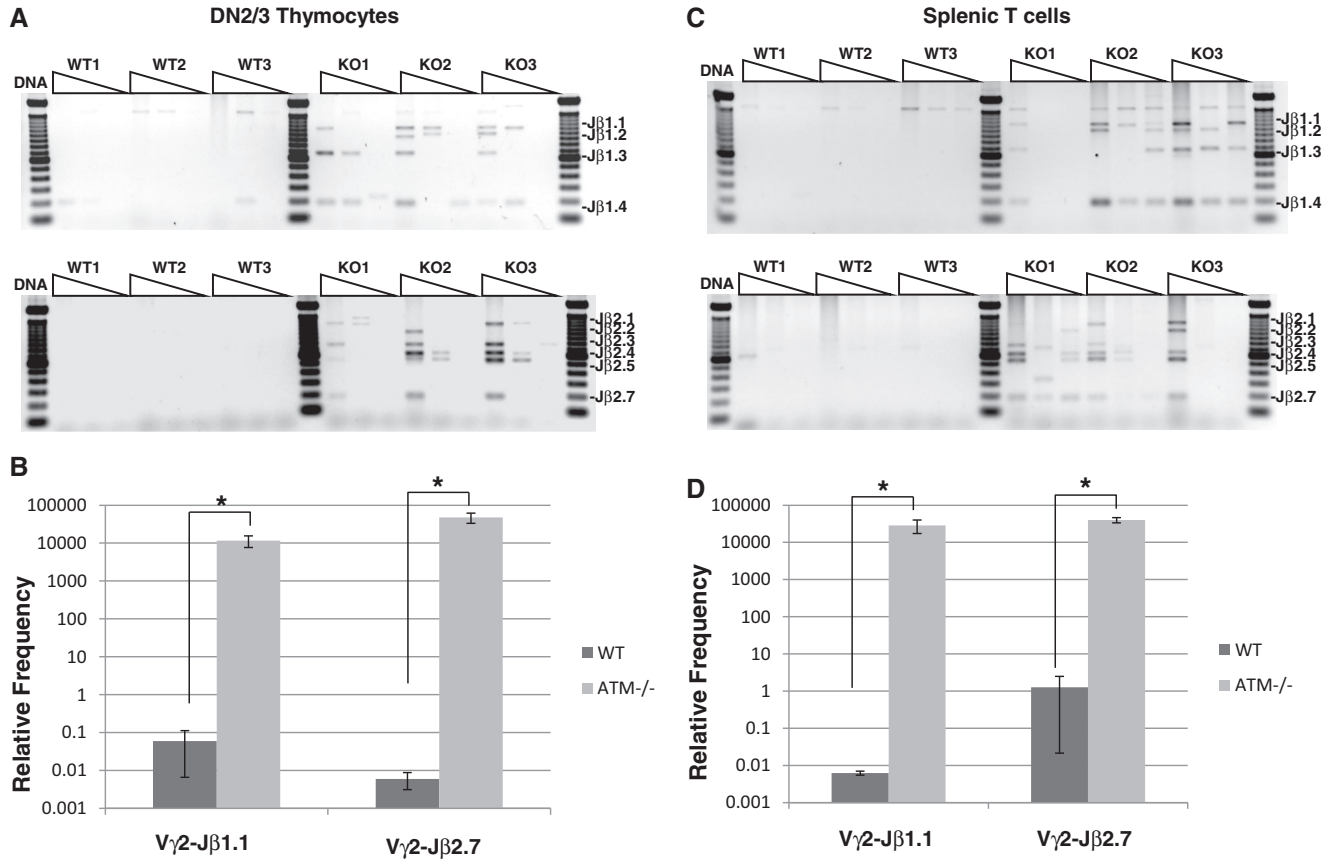

Figure 1. ATM−/− T lymphocytes exhibit an increased frequency of Vγ2–Jβ *trans*-rearrangement. (**A** and **C**) 100, 20 and 4 ng of genomic DNA from DN2/3 thymocytes or splenic T cells was PCR amplified with primers specific for Vγ2 and either the genomic region 3′ of Jβ1.4 or the genomic region 3′ of Jβ2.7. Products were run on a 1.2% agarose gel and stained with ethidium bromide to visualize DNA. (**B** and **D**) Real-time PCR analysis of *trans*-rearrangements between Vγ2 and either Jβ1.1 or Jβ2.7. Data are a summary of three independent experiments. Statistical significance was determined using a student's 2-tailed *t*-test. $*P < 0.05$.

such foci remain intact in ATM-deficient cells in contrast to others, such as γH2AX (23).

We found that ∼12% of sorted WT DN2/DN3 thymocytes contained at least one 53BP1 focus, indicating the presence of DNA damage, and that this percentage was increased ∼2-fold in ATM−/− DN2/DN3 thymocytes (Figure 3A and B). This is consistent with a greater persistence of DSB in the absence of ATM, as has been previously reported (22,24,25). More than 90% of 53BP1 foci co-localized with one of the three TCR loci in both WT and ATM−/− samples. TCRβ, TCRγ and TCRγ all had a similar frequency of co-localization with 53BP1 in WT (∼4–6% of cells) and ATM−/− (∼9–11% of cells) DN2/DN3 thymocytes (Figure 3C and D). Analysis of Rag1−/− and ATM−/−Rag1−/− DN2/3 thymocytes revealed a ∼10-fold reduction in the frequency of cells with 53BP1 foci compared with the WT and ATM−/− samples, respectively. None of the 53BP1 foci found in the Rag1-deficient samples co-localized with TCR FISH signals. This indicates that nearly all of the 53BP1 foci present in DN2/3 thymocytes are due to RAG activity, and not because of other forms of spontaneous DNA damage (Figure 3B).

A fraction of cells contained 53BP1 foci at multiple TCR loci simultaneously, suggesting concurrent V(D)J rearrangement. In the WT sample, simultaneous 53BP1 foci were present at each combination of two TCR loci (TCRβ and TCRγ, TCRβ and TCRδ, TCRγ and TCRδ) at a frequency of 0.4–0.8% of total cells, whereas in ATM−/− cells, this frequency was substantially higher at 1.5–2.0% (Figure 4A and B), again consistent with defective resolution of TCR-associated DNA breaks in ATM−/− T cells. A smaller subpopulation of cells had 53BP1 foci simultaneously at all three TCR loci (∼0.2% in WT, ∼0.65% in ATM−/−) (Figure 4A and B).

If the three TCR loci rearrange independent of one another (with the presence of rearrangement at one locus having no effect on the probability of rearrangement at the other two), then the presence of rearrangement at multiple TCR loci simultaneously in the same cell would be due to random coincidence. If this were the case, the expected frequency of cells with 53BP1 at multiple TCR loci simultaneously can be calculated by multiplying the frequency of cells with 53BP1 at one locus (shown in Figure 3D) by the frequency of cells with 53BP1 at another locus. This calculation gives the frequency of cells with 53BP1 at multiple TCR loci that would be expected if the probability of rearrangement was completely independent for each locus. Figure 4B shows the calculated expected frequency (black horizontal lines) of

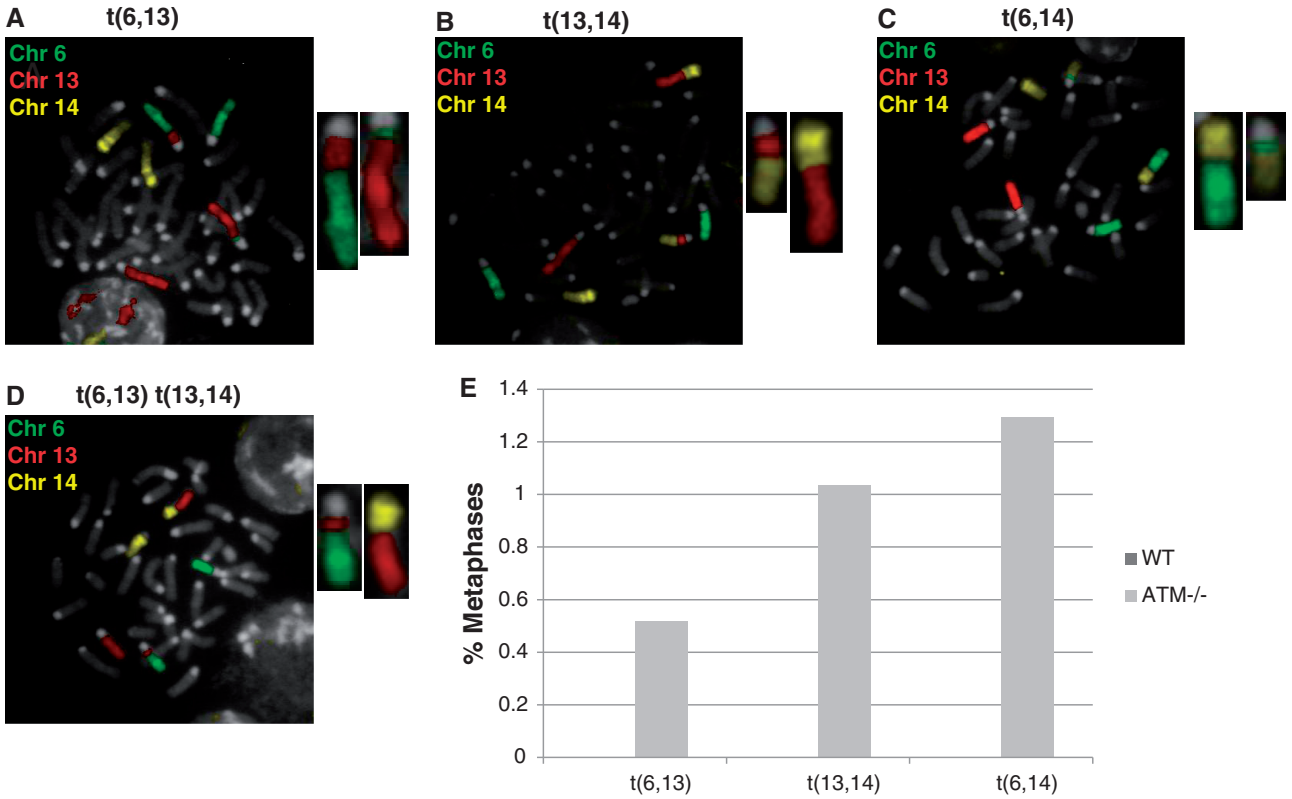

Figure 2. *Trans*-rearrangements result in chromosomal translocations in ATM−/− T cells. Splenic T cells from WT and ATM−/− mice were stimulated *in vitro* with an antibody to CD3 (2C11), and metaphases were prepared. Chromosomes 6, 13 and 14 were hybridized with whole chromosome paint. Translocations were detected in the ATM−/− samples between chromosomes 6 and 13 (**A**), 13 and 14 (**B**) and 6 and 14 (**C**), and the frequency was determined (**E**). Some metaphases carried multiple translocations (**D**). No translocations were detected in the WT sample. Data are representative of two independent experiments in which >1000 metaphases were scored for each genotype.

simultaneous 53BP1 foci at each combination of TCR loci, against the observed frequency shown by the histogram bars. In all cases, the observed frequency of simultaneous rearrangement in both WT and ATM−/− cells was 1.5- to 2-fold greater than the expected frequency (significance at <0.0001 by χ^2 analysis), suggesting that rearrangement is more likely to be initiated at a given locus in cells where rearrangement is already ongoing at another locus than in cells where it is not (Figure 4B). This could reflect heterogeneity within the DN2/DN3 population in terms of locus accessibility or RAG expression, resulting in a subset of cells more likely to undergo recombination than others.

TCR loci do not exhibit subnuclear proximity in DN2/DN3 thymocytes

It has been reported that loci prone to chromosomal translocations tend to occupy the same subnuclear space as their translocation partner in cell types in which they occur (26–28). Using a 3D FISH (3D FISH) approach, we investigated whether, in addition to being simultaneously broken in a subset of DN2/DN3 thymocytes, the TCR loci also tend to be found in closer proximity to one another within the nucleus than to a control locus (actin), which could further predispose to interchromosomal *trans*-rearrangement. Fluorescently labeled probes for each TCR locus, as well as the β-actin locus on chromosome 5 were hybridized to sorted DN2/DN3 thymocytes from WT and ATM−/− mice, and distances between loci were calculated (Figure 5A).

For each cell analyzed, all inter-TCR (TCRβ–TCRγ, TCRβ–TCRδ and TCRγ–TCRδ) as well as control (TCRβ–actin, TCRγ–actin and TCRδ–actin) distances between probes were calculated, and the average of the four calculated distances for each locus pair was used to represent the value for that individual cell. The average distance was then calculated for each interaction for WT and ATM−/− cells. No significant difference was detected between inter-TCR distances and distances between TCR loci and actin (Figure 5B). Furthermore, no significant differences were observed between WT and ATM−/− samples in any of these distances (Figure 5B). These results suggest that the three TCR loci are not localized closer to each other within the DN2/3 nucleus relative to other non-antigen receptor loci that do not participate in translocations and that ATM-deficiency does not alter the overall subnuclear proximity of TCR loci.

Although ATM deficiency did not affect average distances between TCR loci, it remained possible that ATM suppresses chromosomal translocations by selectively preventing close-range interactions between loci when DSBs are present. To test this, we analyzed the frequency of DN2/3 cells with closest inter-TCR distances (<1 μm). We reasoned that if ATM was keeping the TCR loci spatially separated, ATM−/− DN2/3 cells

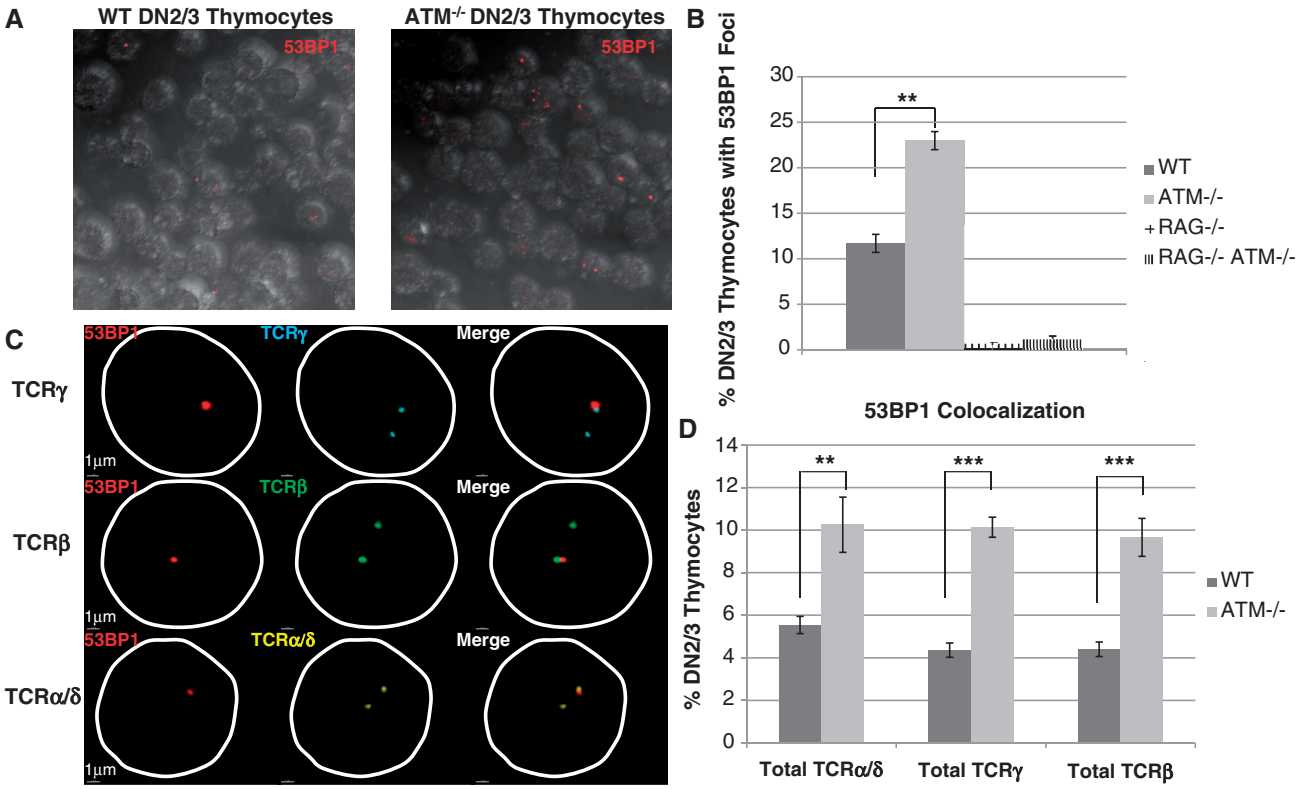

Figure 3. The 53BP1 foci are present at TCR loci in DN2/3 thymocytes. (**A**) DN2/3 thymocytes stained with anti-53BP1 show foci marking sites of DNA DSBs. (**B**) The per cent of cells with 53BP1 foci is shown for WT, ATM−/−, Rag1−/− and ATM−/− Rag1−/− DN2/3 thymocytes. (**C**) Fluorescently labeled BAC probes for the TCRα/δ, TCRβ and TCRγ loci were hybridized to interphase DN2/3 cells in addition to 53BP1 staining. The 53BP1 foci are present at TCR loci. Three examples of cells with 53BP1 foci TCR loci are shown. Top: TCRγ; Middle: TCRβ; Bottom: TCRα//δ. (**D**) The percentage of total DN2/3 thymocytes with TCR FISH signals co-localized with 53BP1 foci. More than 1000 cells were counted in three independent experiments. Statistical significance was determined using a student's two-tailed *t*-test. $*P < 0.05$, $**P < 0.01$, $***P < 0.001$.

might have a higher frequency of interactions within this close range. However, we found no significant difference between WT and ATM−/− cells as analyzed by Wilcoxon rank-sum statistical test (data not shown).

Synaptic complexes form between TCRβ and TCRγ RSSs *in vitro*

In addition to the differing length of spacers that direct pairing of rearranging RSSs (12/23 rule), there are additional features within the conserved heptamer and nonamer as well as within the coding flank of the gene segment that determine RAG-binding affinity, synaptic complex formation and consequently the compatibility of recombination partners (beyond 12/23 rule) (29,30). For instance, despite having compatible spacers, the TCR Vβ and Jβ genes never undergo rearrangement *in vivo*, whereas Dβ and Jβ do (30). It was, therefore, of interest to determine whether *trans*-rearrangement could be mediated by direct interaction between TCR Dβ and TCR Jγ RSSs. We constructed artificial recombination substrates with the 3′-Dβ1 23 RSS cloned upstream of two 12 RSSs derived from Jβ2.5, 5′-Dβ1 and Jγ1 genes (Figure 6A). When co-transfected with Rag1 and Rag2 into HEK 293 cells, two 12 RSSs compete for recombination to the 23 RSS. We found that the 3′-Dβ1 23 RSS rearranges equally to the Jγ1 12 RSS and the Jβ2.5 12 RSS (Figure 6B). Furthermore, the Jγ1 12 RSS dominates rearrangement compared with the 5′-Dβ1 12 RSS (which does not frequently rearrange to the 3′-Dβ1 23 RSS) similar to the Jβ2.5 12 RSS (Figure 6B). These data suggest that not only is synaptic complex formation possible between TCR Dβ and TCR Jγ RSSs but that it is also as efficient as with endogenously rearranging Jβ RSSs. The finding of RSS compatibility is consistent with the model that *trans*-rearrangement, at least in part, may be driven by formation of synaptic complexes in *trans* between two different TCR loci in ATM−/− thymocytes.

Trans-rearrangement occurs in 12/23 and non-12/23 pairs with equal frequency *in vivo*

The observation that the frequency of *trans*-recombination is increased 10 000- to 100 000-fold by ATM deficiency, whereas the increase in persisting DNA damage foci is increased to a far lesser extent, suggested that ATM function may extend beyond the resolution of DNA breaks and break foci. We, therefore, explored the possibility that *trans*-rearrangement might result from instability of post-cleavage *cis* synaptic complexes in the absence of ATM, allowing the broken DNA ends following RAG-mediated cleavage to fall out of the synaptic complex and undergo joining in *trans* (13). If this were the case, *trans*-rearranged products would occur entirely

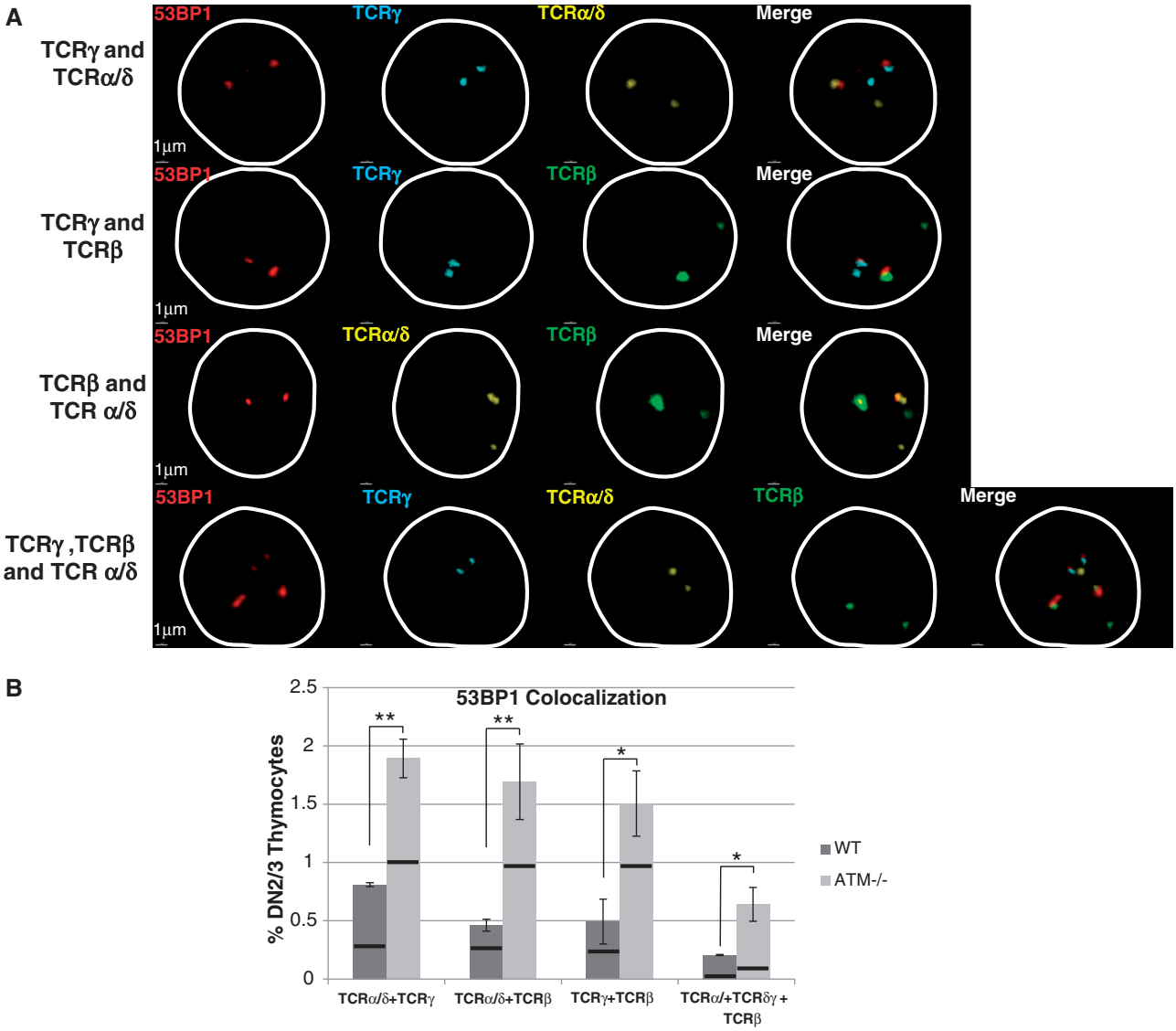

Figure 4. DNA damage foci occur at multiple TCR loci simultaneously in DN2/3 thymocytes. (**A**) ImmunoFISH analysis of 53BP1 focuses co-localization with TCR loci. A subset of DN2/3 thymocytes exhibits multiple 53BP1 foci, each co-localizing with a different TCR locus. (**B**) The percentage of total DN2/3 thymocytes with 53BP1 foci at multiple TCR loci. More than 1000 cells were counted in three independent experiments. Statistical significance was determined using a student's two-tailed *t*-test ($*P < 0.05$, $**P < 0.01$, $***P < 0.001$). χ^2 analysis reveals that the observed frequency of simultaneous foci at multiple TCR loci is significantly greater than expected based on the frequency for each locus individually (shown as black horizontal bars, $P < 0.0001$).

independent of the 12/23 rule, as no synaptic complex formation would be required between the rearranging RSSs in *trans*. To test this, we PCR amplified genomic DNA of WT and ATM−/− DN2/3 thymocytes for *trans*-rearrangements between Jγ1 and the 5′-end of Dβ1 or multiple Jβ gene segments, all of which are flanked with 12 RSSs (Table1), as well as *trans*-rearrangements between the 3′-end of Dβ1, Dβ2 and Vγ2 genes, all of which are flanked with 23 RSSs (Table 2). We readily detected such *trans*-rearrangements in the WT and ATM−/− samples. The junctional sequences of these rearrangements resemble normal *cis* V(D)J junctions with N nucleotide additions and small deletions in the coding flank of both TCRβ and TCRγ genes (Tables 1 and 2). Interestingly, within the Jγ1–Jβ amplifications, rearrangements were present both directly between Jγ1 and Jβ genes as well as between Jγ1 and the 5′-end of Dβ, suggesting that *trans*-rearrangement can occur during attempted Dβ–Jβ rearrangement as well as Vβ–DβJβ rearrangement (Table 1). One sequence contained a large portion of the Jβ1.3 RSS at the Jγ1–Jβ1.3 junction indicating off-target RAG cleavage activity. These 12/23 rule violations during *trans*-rearrangement strongly suggest that these particular rearrangements occur without synaptic complex formation in *trans*.

It was important to determine whether 12/12 or 23/23 *trans*-rearrangements are rare events relative to 12/23 *trans*-rearrangements, or whether these are frequent events that might reflect a common mechanism of *trans*-rearrangement that is independent of RAG-dependent

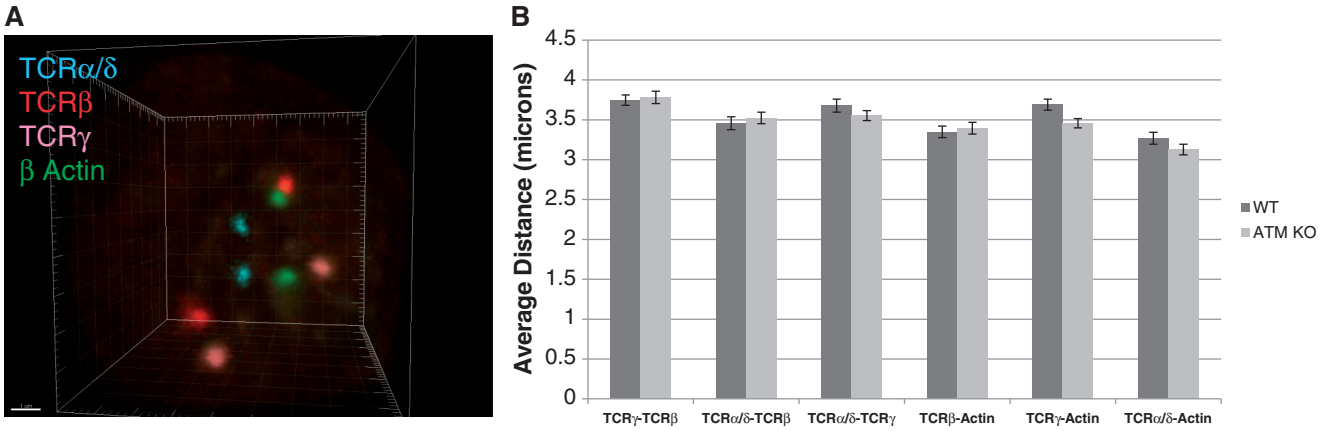

Figure 5. TCR loci are not in preferential spatial proximity in DN2/3 thymocytes. (**A**) Fluorescently labeled DNA probes for the TCRα/δ, TCRβ, TCRγ and β-actin loci were hybridized to sorted interphase DN2/3 thymocytes, and distances between spots were calculated. (**B**) Average interlocus distances (in micrometer) are shown for WT and ATM−/− cells. Data are representative of three independent experiments in which 75–150 nuclei were scored for each genotype. Data were analyzed with a student's two-tailed *t*-test.

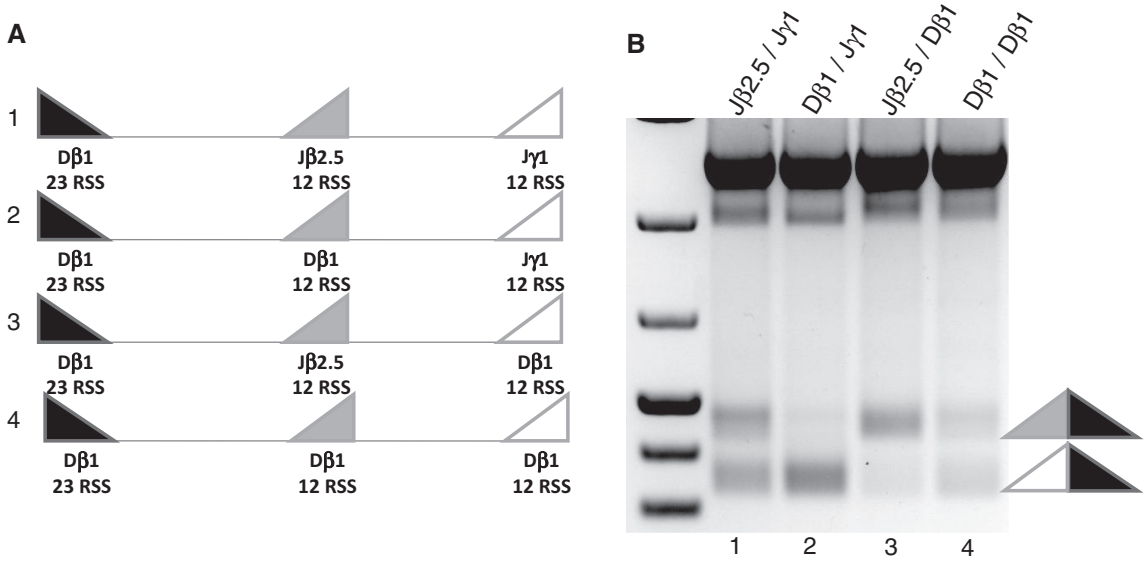

Figure 6. Synaptic complexes form between RSSs of TCRβ and TCRγ. (**A**) Artificial recombination substrates were constructed containing one 23-bp RSS from Dβ1 oriented upstream of two 12-bp RSSs of various combinations. Each construct was transfected separately into HEK 293 cells along with Rag1 and Rag2. (**B**) The recombined products from each construct were PCR amplified and run on a sieving agarose gel. The upper and lower bands represent rearrangements to the proximal and distal RSSs, respectively.

trans-synaptic requirements. To address this question, we used real-time PCR to compare the frequency of Jγ1–Jβ2.7 (12/12) *trans*-rearrangements to Vγ2–Jβ2.7 (12/23) *trans*-rearrangements in three WT and three ATM−/− genomic DNA samples purified from sorted DN2/DN3 thymocytes. A 20-cycle pre-amplification using either Jγ1- or Vγ2-specific forward primer and a reverse primer downstream of Jβ2.7 was required to improve the sensitivity of the assay. We quantified real-time PCR assays using a standard curve derived from serially diluted plasmids containing known copy numbers of either a Jγ1–Jβ2.7 *trans*-rearrangement sequence or a Vγ2–Jβ2.7 *trans*-rearrangement sequence, and linear regression curve fitting (Figure 7A and B). The qPCR values derived from the WT samples, where *trans*-rearrangements are extremely rare, were below the linear portion of the standard curve and could not be included in the analysis. However, in the ATM−/− samples, we found the frequency of Jγ1–Jβ2.7 *trans*-rearrangements to be similar to that of Vγ2–Jβ2.7 *trans*-rearrangements when normalized to the standard curve (Figure 7C). This indicates that *trans*-rearrangements violating the 12/23 rule occur as frequently as those that do not, supporting a model in which many *trans*-rearrangements occur due to instability of multiple, simultaneous post-cleavage *cis*-synaptic complexes rather than single *trans*-synaptic complexes.

DISCUSSION

During the DN stage of T-cell development, recombination occurs at three TCR loci: TCRβ, TCRγ and

Table 1. The 12/12 *trans*-rearrangements between Jγ and Jβ gene segments

Jγ1	N	Dβ	N	Jβ	
TTGTGAAAACCTGAGCTA				CCGTGGACCCGGGAGGCTGTGTTCTGGAAA	1.3
TTGTGAAAACCTGAGCTA				TCTGGAAA	1.3
TTGTGAAAACCTGA				**AAGATTATTTTTCGG**	1.4
TTGTGAAAACCTGAGCTAT				GTGCAGAAACGCTGTATTTT	2.3
TTGTGAAAACCTGAGCT	CAAACACT			AGTGCAGAAACGCTGTATTTT	2.3
TTGTGAAAACCTG	T			AGTCAAAACACCTTGTACTTT	2.4
TTGTGAAAGCCCGAGC	CATAAAC			TCAAAACACCTTGTACTTT	2.4
TTGTGAAAACCTGAGC	CC			AGTCAAAACACCTTGTACTTT	2.4
TTGTGAAAGCCCGAGCTAT	GA	GGGA	GAGC	GTCAAAACACCTTGTACTTT	2.4
TTGTGAAAACCTGAGCTA	TCCCCCTT			AGTCAAAACACCTTGTACTTT	2.4
TTGTGAAAACCTGAGC	CAC			CCAAGACACCCAGTACTTT	2.5
TTGTGAAAACCTGAGCTAT	ATG	TGGGGGGGGC	CGT	CAAGACACCCAGTACTTT	2.5
TTGTGAAAACCTGAGC	**CCCA**			**TATGAACAGTACTTCGGTCCC**	2.7
TTGTGAAAACCTGAGCTAT	**ATT**			**CAGTACTTCGGTCCC**	2.7
TTGTGAAAACCTGAGCTAT	**ACCC**	**GGGG**	**CTCG**	**CCTATGAACAGTACTTCGGTCCC**	2.7
TTGTGAAA	**GCCCGAGCTATA**			**TCCTATGAACAGTACTTCGGTCCC**	2.7

Junctional sequences of PCR amplified rearrangements between Jγ1 and various Jβ genes are shown. In all, 100 ng of genomic DNA isolated from WT (bold) or ATM−/− DN2/3 cells was used to PCR amplify 12/12 rearrangements using a reverse primer specific for the Jγ1 (GJ1R1) gene and a second reverse primer downstream of either the first (3Jb1b) or second (3Jb2) Jβ clusters. PCR products were purified, cloned into a TA vector and sequenced using M13 universal sequencing primers. Identity of Jβ genes are shown in far right column.

TCRδ. In the present study, we show that DN thymocytes also participate in abnormal *trans*-rearrangements between TCR loci, and that the frequency of these events is greatly increased in ATM-deficient mice. We have further assessed and provided insight into the mechanism underlying these events and the function of ATM in resolution of RAG-dependent TCR breaks. Two fundamentally different, but not mutually exclusive, mechanisms may lead to TCR *trans*-rearrangement. First, formation of a single synaptic complex between two compatible RSS bound with RAG proteins on two different chromosomes in *trans* may result in coordinated cleavage and joining of two different loci resulting in a chromosomal translocation. We tested the possibility of this mechanism directly with an *in vitro* recombination assay and found that at least some combinations of participating RSS from different loci can undergo recombination *in vitro*, which would be a prerequisite for synapsis and cleavage to occur in *trans*. A second possible mechanism is that *trans*-rearrangements occur between simultaneously existing unstable DNA breaks at distinct TCR loci, formed in two traditional *cis* synaptic complexes, independent of any requirement for direct RAG-mediated synapse between these TCR loci. ATM, and several associated DDR components, has been reported to be important in physically stabilizing broken DNA ends in the post-cleavage synaptic complex to prevent improper joining of DNA ends, as evidenced by the presence of abnormal hybrid joints between the coding and signal ends of separate genes in ATM-deficient cells (13,14). Similarly, ATM has been implicated in directing the proper DNA end usage for repair when multiple DNA breaks are present simultaneously (31). Thus, it is possible that instability of two simultaneously formed post-cleavage complexes could result in *trans*-rearrangements with precise junctions, but without the formation of a synaptic complex in *trans*. Our finding that there is no preference for 12/23 *trans*-rearrangement over 12/12 or 23/23 *trans*-rearrangement is consistent with this mechanism, as no direct synapse would be formed between the *trans*-recombining gene segments. The 12/23 rule violations have been described at the IgH and Igκ loci, but they are inefficient and occur at an extremely low frequency (32,33). Translocations violating the 12/23 rule have also been described using retroviral recombination substrates in ATM−/− abl-transformed pre-B cell lines

Table 2. The 23/23 *trans*-rearrangements between Vγ and Dβ gene segments

Vγ2	N	Dβ1
TACTGTTCCTACGGC	TAAAT	CTGTCCC
TACTACTGTTCC	CA	CCCCTGTCCC
TACTGTTTCTACGGC	TCCCGT	CCCTGTCCC
TACTGTTCCTACGG	GAA	CCCTGTCCC
TACTGTTCCTACGGC	TAAATG	GCCCCC
TACTACTGTTCCTACGGC	TAAACGGCA	GTCCC
TACTACTGTTCCTACG	**GACA**	**CCCTGTCCC**

Vγ2	N	Dβ2
TACTGTTCCTACGGC	TAAAAAT	CCCCCAGTCCC
TACTGTTCCTACGG	G	GCCCCCCCAGTCCC
TACTGTTCCTACGGC	TAAAGTTTTGGAT	GCCCCCCCAGTCC
TACTGTTCCTACGGC	TAAT	CCCCCCCAGTCCC
TACTGTTCCTACGGC		CCAGTCCC
TACTGTTCCTACGGC	TAAGCA	CCCCCCAGTCCC
TACTGTTCCTACGGC	TAGGGGA	CCCCCCCAGTCCC
TACTGTTCCTACGGC	TAAAAAT	CCCCCAGTCCC
TACTGTTCCTACGGC	TAAAGGAAGTTTAGGAA	CCCCAGTCCC
TACTGTTCCTACGGC	TAAACAT	CCCCCAGTCCC
TACTGTTCCTACGGC	TAGGGGAC	CCCCCCCAGTCCC
TACTGTTCCTACGGC	TACT	GCCCCCCCCAGTCCC
TACTGTTCCTACGGC	**TT**	**GCCCCCCCAGTCCC**
TACTGTTCCTACG	**TAAGGC**	**CCCCCCAGTCCC**
TACTGTTCCTACGGC	**TACCGGC**	**CCCCAGTCCC**

Junctional sequences of PCR amplified rearrangements between Vγ2 and the 3′-end of Dβ1 or Dβ2 are shown. In all, 100 ng of genomic DNA isolated from WT (bold) or ATM−/− DN2/3 cells was used to PCR amplify 23/23 rearrangements using a forward primer specific for theVγ2 gene (GV4F1) and a second forward primer upstream of either Dβ1 (5Db1SE) or Dβ2 (5Db2SE). PCR products were purified, cloned into a TA vector and sequenced using M13 universal sequencing primers.

(34). The *trans*-rearrangements we have observed in violation of the 12/23 rule also seem to have joints with features of normal *cis* V(D)J rearrangements, such as N nucleotide additions and small deletions in the coding ends, and occur at a frequency similar to that of *trans*-rearrangements that obey the 12/23 rule. This suggests that *trans*-rearrangements with normal features can be formed without the dependence on *bona fide trans*-synaptic complex formation. Although we cannot rule out that some 12/23 *trans*-rearrangements may occur via synaptic complexes in *trans* between two chromosomes, we suggest that the marked instability of post-cleavage synaptic complexes, combined with an increased frequency of simultaneous breaks, is largely responsible for the dramatically elevated frequency of *trans*-rearrangement in ATM deficiency.

TCR *trans*-rearrangement has been studied previously in humans and mice as a consequence of genomic instability in multiple contexts (10–12,35,36). Patients with AT have an increased frequency of *trans*-rearrangements in their peripheral T cells compared with normal individuals (10,11). Healthy agricultural workers, exposed to certain genotoxic chemicals, also carry a significantly higher frequency of *trans*-rearrangements than unexposed individuals (35). To the same effect, it has been found that irradiation drastically increases the rate of *trans*-rearrangement in SCID mice, who have a genetic defect in DNA end-joining (36). *Trans*-rearrangements are chromosomal translocations that have been identified in human lymphoid malignancies (37) and presumably occur through a similar mechanism to other oncogenic translocations. Indeed, it has been proposed that perhaps all antigen receptor locus-associated oncogenic translocations are the result of aberrant V(D)J recombination and/or class switch recombination and somatic hypermutation (38). Therefore, we chose to study *trans*-rearrangement between three recombining TCR loci as a model of chromosomal translocations in ATM-deficient mice. TCR *trans*-rearrangements offer the advantage over random chromosome translocations of occurring at high

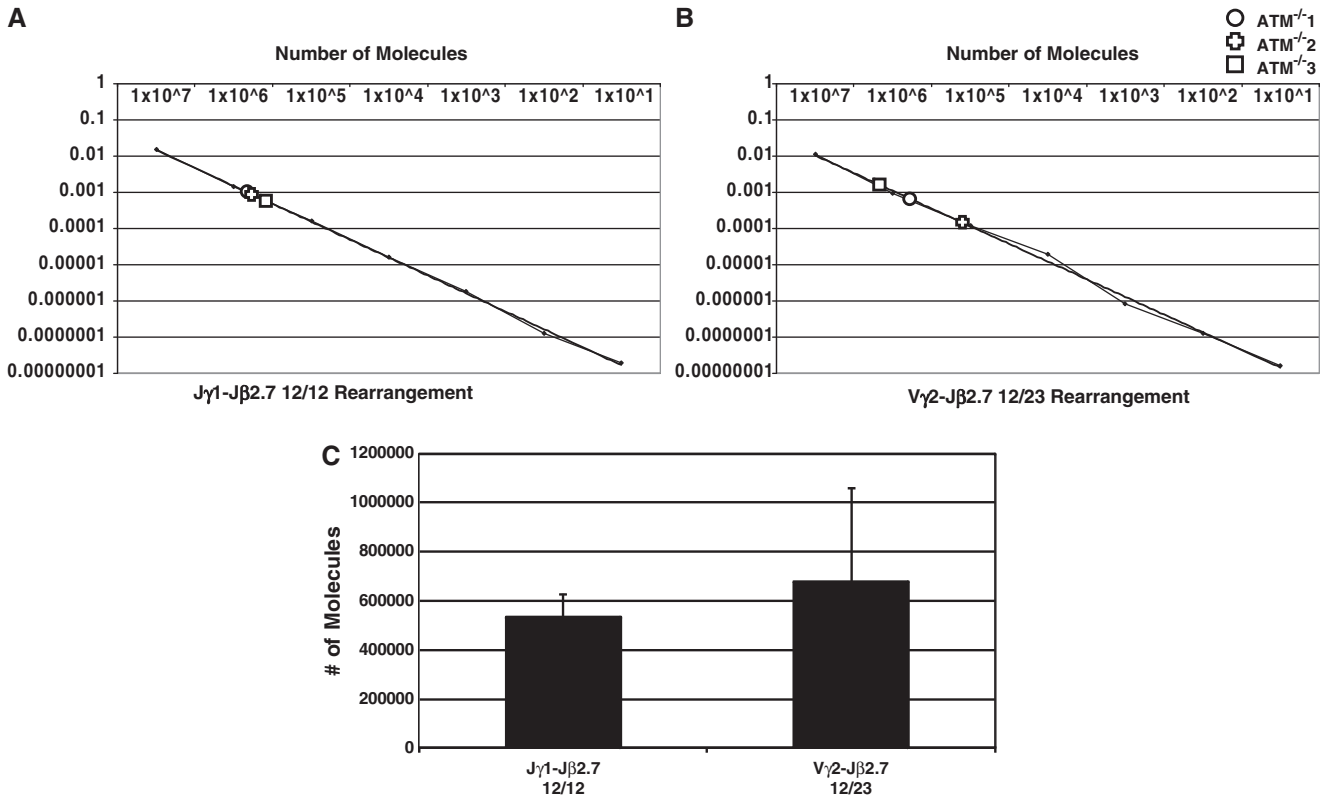

Figure 7. The 12/12 and 12/23 *trans*-rearrangements occur at a similar frequency in DN2/DN3 thymocytes real-time PCR analysis of Jγ1–Jβ2.7 (**A**) or Vγ2–Jβ2.7 (**B**) *trans*-rearrangements. Pre-amplified genomic DNA from DN2/DN3 thymocytes of ATM−/− mice was used as a template, and experimental values were fitted to a standard curve of 10-fold serially diluted constructs containing *trans*-rearrangement sequences. (**C**) The number of molecules corresponding to each individual sample was calculated using linear regression analysis and averaged for both Jγ1–Jβ2.7 and Vγ2–Jβ2.7 *trans*-rearrangements. Each DNA sample was obtained from a pool of five to seven individual mice.

frequency (>1%) in a known cell type and developmental stage (DN2/3 thymocytes) with well-defined breakpoints that are easily detectable by PCR.

Spatial proximity and temporal coincidence of DNA DSBs are thought to be the two major factors contributing to recurrent chromosomal translocations, but the relative importance of each factor remains controversial. The arrangement of chromosomes within the interphase nuclei of specific cell types is non-random, in that certain chromosomes tend to occupy distinct subnuclear territories (39). Thus, genes on different chromosomes could have a preferential spatial proximity in the nucleus that might predispose them to translocation if simultaneously broken (27,28,40). In our study, we used ImmunoFISH to evaluate the frequency of simultaneous DNA DSB foci in DN2/3 thymocytes at multiple TCR loci and 3D FISH to measure the physical distances between TCR loci to assess the contribution of DSB formation and spatial proximity to *trans*-rearrangement. We analyzed co-localization of 53BP1 with the TCR loci to estimate the frequency of cells rearranging a given locus at a particular time. We found that the frequency of total DN2/3 thymocytes with simultaneous break foci at multiple loci is increased 2- to 3-fold for each locus combination in ATM−/− mice. This phenotype is consistent with a defect in the timely repair of DNA damage in the absence of ATM, which results in persistent DNA breaks (22,24,41) and a higher frequency of cells with 53BP1 foci. An alternative interpretation of these results would be that there is a delay in disassembly of 53BP1 foci in the absence of ATM rather than a delay in DNA break repair. This interpretation, however, is inconsistent with a previous report showing that persistence of DNA damage foci in ATM-deficient cells correlates with persistence of damaged DNA (25).

The 2- to 3-fold increase in the frequency of simultaneous DSB at multiple TCR loci in the absence of ATM does not fully predict the dramatically (10 000- to 100 000-fold) higher frequency of *trans*-rearrangements. A factor that could potentially contribute to the frequency of *trans*-rearrangement would be preferential co-localization of TCR loci in the interphase nucleus, where rearrangement is taking place. However, our 3D FISH analysis revealed no detectable difference in the average distance between the TCR loci in WT and ATM−/− cells. Furthermore, the inter-TCR distances were not significantly closer than distances between TCR loci and the β-actin locus, which does not rearrange or participate in known translocations. These data suggest that the TCR loci in the interphase nucleus of DN2/3 cells are not in preferential proximity to each other relative to the actin control, and that the absence of ATM does not substantially alter subnuclear proximity of the rearranging TCR loci relative to each other.

Two recent studies have provided insight into the relative contributions of DNA damage and spatial proximity to chromosomal translocations (42,43). When translocations occur due to low-frequency random DNA DSBs, targeting is proportional to the spatial proximity of the rearranging loci. In contrast, DNA DSBs induced at high frequencies by developmentally programmed mechanisms, such as V(D)J recombination (43) or AID-associated mutations (42), dictate translocations predominantly to antigen receptor loci where the most DNA damage occurs. TCR *trans*-rearrangement in DN2/3 thymocytes clearly falls into the latter category as we demonstrate that the RAG proteins induce simultaneous DNA DSB foci at TCR loci, which can undergo low-frequency *trans*-rearrangement, even in WT cells. We have found no evidence of translocations other than those explained by TCR *trans*-rearrangement in WT thymocytes. Although the frequency of *trans*-rearrangement increases drastically in ATM−/− cells, there is no increase in proximity between TCR loci, consistent with the notion that elevated translocation targeting between the TCR loci is due to increased DNA damage (as a consequence of delayed DSB repair and defective DNA end stability) as opposed to altered subnuclear localization. This conclusion differs from another recent report, proposing that ATM plays a role in maintaining allele separation during immunoglobulin locus recombination in pre-pro B cells (16). We find no evidence for a role of ATM in enforcing a general spatial separation of TCR loci in DN2/3 thymocytes, nor in the specific prevention of close spatial interactions of $<1\,\mu M$, despite the observation that such *trans*-rearrangements create heterologous interchromosomal translocations. Another DDR protein, 53BP1, has also been implicated in large-scale chromosome organization during V(D)J recombination (44) and class switch recombination (45) raising the possibility that the DDR pathway in general contributes to the shape and organization of the interphase nucleochromatin. However, our data show that whatever this contribution may be, the most critical function of ATM in suppressing chromosomal translocations during V(D)J recombination is to prevent prolonged unrepaired DNA damage and to maintain the physical stability of the post-cleavage synaptic complex regardless of their overall position in the nucleus.

SUPPLEMENTARY DATA

Supplementary Data are available at NAR Online: Supplementary Table 1 and Supplementary Figure 1.

ACKNOWLEDGEMENTS

Special thanks to Mike Kruhlak for microscopy support, Larry Granger for cell sorting and Henry Chen for technical advice. The authors also thank Andre Nussenzweig and Martin Gellert for helpful discussion of the results and Seth Steinberg for invaluable help with statistical analysis.

FUNDING

Intramural Research Program of the National Institutes of Health. The funders had no role in study design, data collection and analysis, decision to publish or preparation of the manuscript. Funding for open access charge: National Institutes of Health intramural program.

Conflict of interest statement. None declared.

REFERENCES

1. Schatz,D.G. and Swanson,P.C. (2011) V(D)J recombination: mechanisms of initiation. *Annu. Rev. Genet.*, **45**, 167–202.
2. Hiom,K. and Gellert,M. (1998) Assembly of a 12/23 paired signal complex: a critical control point in V(D)J recombination. *Mol. Cell*, **1**, 1011–1019.
3. van Gent,D.C., Ramsden,D.A. and Gellert,M. (1996) The RAG1 and RAG2 proteins establish the 12/23 rule in V(D)J recombination. *Cell*, **85**, 107–113.
4. Tonegawa,S. (1983) Somatic generation of antibody diversity. *Nature*, **302**, 575–581.
5. Livák,F., Tourigny,M., Schatz,D.G. and Petrie,H.T. (1999) Characterization of TCR gene rearrangements during adult murine T cell development. *J. Immunol.*, **162**, 2575–2580.
6. Taylor,A.M., Metcalfe,J.A., Thick,J. and Mak,Y.F. (1996) Leukemia and lymphoma in ataxia telangiectasia. *Blood*, **87**, 423–438.
7. Callén,E., Bunting,S., Huang,C.Y., Difilippantonio,M.J., Wong,N., Khor,B., Mahowald,G., Kruhlak,M.J., Ried,T., Sleckman,B.P. *et al.* (2009) Chimeric IgH-TCRalpha/delta translocations in T lymphocytes mediated by RAG. *Cell Cycle*, **8**, 2408–2412.
8. Liyanage,M., Weaver,Z., Barlow,C., Coleman,A., Pankratz,D.G., Anderson,S., Wynshaw-Boris,A. and Ried,T. (2000) Abnormal rearrangement within the alpha/delta T-cell receptor locus in lymphomas from Atm-deficient mice. *Blood*, **96**, 1940–1946.
9. Aurias,A., Dutrillaux,B., Buriot,D. and Lejeune,J. (1980) High frequencies of inversions and translocations of chromosomes 7 and 14 in ataxia telangiectasia. *Mutat. Res.*, **69**, 369–374.
10. Kobayashi,Y., Tycko,B., Soreng,A.L. and Sklar,J. (1991) Transrearrangements between antigen receptor genes in normal human lymphoid tissues and in ataxia telangiectasia. *J. Immunol.*, **147**, 3201–3209.
11. Lipkowitz,S., Stern,M.H. and Kirsch,I.R. (1990) Hybrid T cell receptor genes formed by interlocus recombination in normal and ataxia-telangiectasis lymphocytes. *J. Exp. Med.*, **172**, 409–418.
12. Stern,M.H., Lipkowitz,S., Aurias,A., Griscelli,C., Thomas,G. and Kirsch,I.R. (1989) Inversion of chromosome 7 in ataxia telangiectasia is generated by a rearrangement between T-cell receptor beta and T-cell receptor gamma genes. *Blood*, **74**, 2076–2080.
13. Bredemeyer,A.L., Sharma,G.G., Huang,C.Y., Helmink,B.A., Walker,L.M., Khor,K.C., Nuskey,B., Sullivan,K.E., Pandita,T.K., Bassing,C.H. *et al.* (2006) ATM stabilizes DNA double-strand-break complexes during V(D)J recombination. *Nature*, **442**, 466–470.
14. Helmink,B.A., Bredemeyer,A.L., Lee,B.S., Huang,C.Y., Sharma,G.G., Walker,L.M., Bednarski,J.J., Lee,W.L., Pandita,T.K., Bassing,C.H. *et al.* (2009) MRN complex function in the repair of chromosomal Rag-mediated DNA double-strand breaks. *J. Exp. Med.*, **206**, 669–679.
15. Matei,I.R., Guidos,C.J. and Danska,J.S. (2006) ATM-dependent DNA damage surveillance in T-cell development and leukemogenesis: the DSB connection. *Immunol. Rev.*, **209**, 142–158.
16. Hewitt,S.L., Yin,B., Ji,Y., Chaumeil,J., Marszalek,K., Tenthorey,J., Salvagiotto,G., Steinel,N., Ramsey,L.B., Ghysdael,J. *et al.* (2009) RAG-1 and ATM coordinate monoallelic recombination and nuclear positioning of immunoglobulin loci. *Nat. Immunol.*, **10**, 655–664.

17. Barlow,C., Hirotsune,S., Paylor,R., Liyanage,M., Eckhaus,M., Collins,F., Shiloh,Y., Crawley,J.N., Ried,T., Tagle,D. *et al.* (1996) Atm-deficient mice: a paradigm of ataxia telangiectasia. *Cell*, **86**, 159–171.
18. Ried,T., Baldini,A., Rand,T.C. and Ward,D.C. (1992) Simultaneous visualization of seven different DNA probes by in situ hybridization using combinatorial fluorescence and digital imaging microscopy. *Proc. Natl Acad. Sci. USA*, **89**, 1388–1392.
19. Wangsa,D., Heselmeyer-Haddad,K., Ried,P., Eriksson,E., Schäffer,A.A., Morrison,L.E., Luo,J., Auer,G., Munck-Wikland,E., Ried,T. *et al.* (2009) Fluorescence in situ hybridization markers for prediction of cervical lymph node metastases. *Am. J. Pathol.*, **175**, 2637–2645.
20. Chen,H.T., Bhandoola,A., Difilippantonio,M.J., Zhu,J., Brown,M.J., Tai,X., Rogakou,E.P., Brotz,T.M., Bonner,W.M., Ried,T. *et al.* (2000) Response to RAG-mediated VDJ cleavage by NBS1 and gamma-H2AX. *Science*, **290**, 1962–1965.
21. Sayegh,C.E., Jhunjhunwala,S., Riblet,R. and Murre,C. (2005) Visualization of looping involving the immunoglobulin heavy-chain locus in developing B cells. *Genes Dev.*, **19**, 322–327.
22. Callén,E., Jankovic,M., Difilippantonio,S., Daniel,J.A., Chen,H.T., Celeste,A., Pellegrini,M., McBride,K., Wangsa,D., Bredemeyer,A.L. *et al.* (2007) ATM prevents the persistence and propagation of chromosome breaks in lymphocytes. *Cell*, **130**, 63–75.
23. Schultz,L.B., Chehab,N.H., Malikzay,A. and Halazonetis,T.D. (2000) p53 binding protein 1 (53BP1) is an early participant in the cellular response to DNA double-strand breaks. *J. Cell Biol.*, **151**, 1381–1390.
24. Huang,C.Y., Sharma,G.G., Walker,L.M., Bassing,C.H., Pandita,T.K. and Sleckman,B.P. (2007) Defects in coding joint formation in vivo in developing ATM-deficient B and T lymphocytes. *J. Exp. Med.*, **204**, 1371–1381.
25. Riballo,E., Kühne,M., Rief,N., Doherty,A., Smith,G.C., Recio,M.J., Reis,C., Dahm,K., Fricke,A., Krempler,A. *et al.* (2004) A pathway of double-strand break rejoining dependent upon ATM, Artemis, and proteins locating to gamma-H2AX foci. *Mol. Cell*, **16**, 715–724.
26. Wang,J.H., Gostissa,M., Yan,C.T., Goff,P., Hickernell,T., Hansen,E., Difilippantonio,S., Wesemann,D.R., Zarrin,A.A., Rajewsky,K. *et al.* (2009) Mechanisms promoting translocations in editing and switching peripheral B cells. *Nature*, **460**, 231–236.
27. Meaburn,K.J., Misteli,T. and Soutoglou,E. (2007) Spatial genome organization in the formation of chromosomal translocations. *Semin. Cancer Biol.*, **17**, 80–90.
28. Roix,J.J., McQueen,P.G., Munson,P.J., Parada,L.A. and Misteli,T. (2003) Spatial proximity of translocation-prone gene loci in human lymphomas. *Nat. Genet.*, **34**, 287–291.
29. Olaru,A., Petrie,H.T. and Livák,F. (2005) Beyond the 12/23 rule of VDJ recombination independent of the Rag proteins. *J. Immunol.*, **174**, 6220–6226.
30. Bassing,C.H., Alt,F.W., Hughes,M.M., D'Auteuil,M., Wehrly,T.D., Woodman,B.B., Gärtner,F., White,J.M., Davidson,L. and Sleckman,B.P. (2000) Recombination signal sequences restrict chromosomal V(D)J recombination beyond the 12/23 rule. *Nature*, **405**, 583–586.
31. Bennardo,N. and Stark,J.M. (2010) ATM limits incorrect end utilization during non-homologous end joining of multiple chromosome breaks. *PLoS Genet.*, **6**, e1001194.
32. Koralov,S.B., Novobrantseva,T.I., Hochedlinger,K., Jaenisch,R. and Rajewsky,K. (2005) Direct in vivo VH to JH rearrangement violating the 12/23 rule. *J. Exp. Med.*, **201**, 341–348.
33. Vinocur,J.M., Fesnak,A.D., Liu,Y., Charan,D. and Prak,E.T. (2009) Violations of the 12/23 rule at the mouse immunoglobulin kappa locus, including V kappa-V kappa rearrangement. *Mol. Immunol.*, **46**, 2183–2189.
34. Mahowald,G.K., Baron,J.M., Mahowald,M.A., Kulkarni,S., Bredemeyer,A.L., Bassing,C.H. and Sleckman,B.P. (2009) Aberrantly resolved RAG-mediated DNA breaks in Atm-deficient lymphocytes target chromosomal breakpoints in cis. *Proc. Natl Acad. Sci. USA*, **106**, 18339–18344.
35. Lipkowitz,S., Garry,V.F. and Kirsch,I.R. (1992) Interlocus V-J recombination measures genomic instability in agriculture workers at risk for lymphoid malignancies. *Proc. Natl Acad. Sci. USA*, **89**, 5301–5305.
36. Lista,F., Bertness,V., Guidos,C.J., Danska,J.S. and Kirsch,I.R. (1997) The absolute number of trans-rearrangements between the TCRG and TCRB loci is predictive of lymphoma risk: a severe combined immune deficiency (SCID) murine model. *Cancer Res.*, **57**, 4408–4413.
37. Denny,C.T., Yoshikai,Y., Mak,T.W., Smith,S.D., Hollis,G.F. and Kirsch,I.R. (1986) A chromosome 14 inversion in a T-cell lymphoma is caused by site-specific recombination between immunoglobulin and T-cell receptor loci. *Nature*, **320**, 549–551.
38. Tsai,A.G., Lu,H., Raghavan,S.C., Muschen,M., Hsieh,C.L. and Lieber,M.R. (2008) Human chromosomal translocations at CpG sites and a theoretical basis for their lineage and stage specificity. *Cell*, **135**, 1130–1142.
39. Parada,L. and Misteli,T. (2002) Chromosome positioning in the interphase nucleus. *Trends Cell Biol.*, **12**, 425–432.
40. Soutoglou,E. and Misteli,T. (2008) On the contribution of spatial genome organization to cancerous chromosome translocations. *J. Natl Cancer Inst. Monogr.*, **39**, 16–19.
41. Vacchio,M.S., Olaru,A., Livak,F. and Hodes,R.J. (2007) ATM deficiency impairs thymocyte maturation because of defective resolution of T cell receptor alpha locus coding end breaks. *Proc. Natl Acad. Sci. USA*, **104**, 6323–6328.
42. Hakim,O., Resch,W., Yamane,A., Klein,I., Kieffer-Kwon,K.R., Jankovic,M., Oliveira,T., Bothmer,A., Voss,T.C., Ansarah-Sobrinho,C. *et al.* (2012) DNA damage defines sites of recurrent chromosomal translocations in B lymphocytes. *Nature*, **484**, 69–74.
43. Zhang,Y., McCord,R.P., Ho,Y.J., Lajoie,B.R., Hildebrand,D.G., Simon,A.C., Becker,M.S., Alt,F.W. and Dekker,J. (2012) Spatial organization of the mouse genome and its role in recurrent chromosomal translocations. *Cell*, **148**, 908–921.
44. Difilippantonio,S., Gapud,E., Wong,N., Huang,C.Y., Mahowald,G., Chen,H.T., Kruhlak,M.J., Callen,E., Livak,F., Nussenzweig,M.C. *et al.* (2008) 53BP1 facilitates long-range DNA end-joining during V(D)J recombination. *Nature*, **456**, 529–533.
45. Ward,I.M., Reina-San-Martin,B., Olaru,A., Minn,K., Tamada,K., Lau,J.S., Cascalho,M., Chen,L., Nussenzweig,A., Livak,F. *et al.* (2004) 53BP1 is required for class switch recombination. *J. Cell Biol.*, **165**, 459–464.